Optimization of industrial shortening manufacturing procedure: The effect of cooling rate and kneading parameters on viscoelasticity and sensory properties

Mahnaz Ameli
Islamic Azad University
Leila Roufegarinejad
Islamic Azad University
Azizollaah Zargaraan (zargaran@gmail.com)
Shahid Beheshti University of Medical Sciences
Farid Zayeri
Shahid Beheshti University of Medical Sciences

Research Article

Keywords: Rheology, Crystallization, Shortening, Design of experiment, Storage modulus (G'), Loss modulus (G")

Posted Date: June 1st, 2022

DOI: https://doi.org/10.21203/rs.3.rs-1668483/v1

Abstract

The main objective of this study was to optimize the industrial shortening manufacturing procedure and investigate the effect of cooling rate and kneading parameters on its viscoelasticity and sensory properties The three selected main crystallization process parameters include the third cooling stage outlet temperature (28–31°C), kneading parameter (100–280 RPM), and filling temperature (30–36°C). The design type and model were Box-Behnken and quadratic, respectively. Rheological viscoelastic experiments on 17 samples with different crystallization factors were performed. Cooling and kneading intensities were manipulated in order to explore the resulting changes in frequency and strain sweep parameters. Additionally, sensory attributes related to the crystallization treatment samples were analyzed. The optimum crystallization parameters that led to the most desired functional attributes were crystallizer 3 outlet temperature of 31°C, kneading intensity of 280 RPM, and filling temperature of 33°C. All the storage modulus (G') and the loss modulus (G") model responses exhibited values in the minimum range at the optimum process conditions. This work's framework sets a new guideline for fine-tuning the functional properties of confectionary shortening through underlying the important role of the optimized crystallization process.

1. Introduction

Lipid shortenings are usually composed of a mixture of oils from a number of sources such as un-hydrogenated, partially, and fully hydrogenated oils, as well as emulsifiers, and other additives. Canola, cottonseed, lard, palm, soybean, and tallow are typical edible oils used for the production of shortenings. Because of the relatively high number of influencing factors, it is quite challenging to understand the effect of molecular composition, processing conditions, additives, and emulsifiers on physical functionality (Humphrey, Moquin, and Narine, 2003). One of the significant components in shortenings, margarine, and specialty products are plastic vegetable oils and fats. It is well known that the solid-like behavior of plastic fats is due to the presence of a fat crystal network (Litwinenko et al., 2002). In terms of the rheological analysis, shortenings are semi-plastic materials that are capable of creating the desirable textural properties in fatty-based foods (Hakimzadeh et al., 2020). Moriya et al. investigated the effect of solid fat content on the G' and G" of margarine and found that the G' and G" increased linearly with the increase in the solid fat content in a double-logarithmic plot, independent of the type of margarine (Moriya, Hasome, and Kawai, 2020). Bakery shortening has the ability to impart texture, tenderness, and taste to baked products. Shortening functionality depends on crystallization behavior, melting profile, and viscoelastic properties (Saghafi et al., 2018). Texturizing a shortening to improve its plasticity is usually achieved by a chilling process in which the melted fat is rapidly cooled in a chilling unit. Crystallization under shear not only improves the plasticity and texture of the mixture, it also removes the heat of crystallization from the sample (Ahmadi and Marangoni, 2009; Erickson, 1990). The nature of the crystal network, including its spatial distribution, and the number, size, and shape of its constituent microstructural elements can be dramatically altered by changes in crystallization conditions (Litwinenko et al., 2002). The effect of cooling in a surface scraping heat exchanger system on dynamic fat crystallization and physicochemical properties of puff pastry shortening was studied. The results revealed that crystallization temperature affected the rheological properties as well as the hardness of the produced shortenings (Nguyen et al., 2021). The scraped surface heat exchanger consists of a steel shaft rotating in a tube that is cooled externally by boiling ammonia. The rotating shaft is fitted with scraper blades which at high rotation speeds are pressed against the cooled inner surface by centrifugal force (Haighton, 1969). To minimize the post-crystallization phenomenon in order to ensure the development of the proper crystal structure and desired plasticity, the cooling and working stages must be prolonged (Alexandersen, Ghazani, and Marangoni, 2020; Masuchi et al., 2014). Accessing the desirable texture and functionality of shortenings could be accomplished by some modification processes, including hydrogenation, fractionation, blending, and chemical or enzymatic interesterification of fats and oils (Saghafi et al., 2018). Hydrogenation of unsaturated fatty acids in edible oils allows for the conversion of liquid oils into semi-solid or solid fats. These fats are characterized by altered melting and textural characteristics and a higher oxidative stability (Litwinenko et al., 2002). Ahmed et al. reported the physiochemical properties of a model shortening. Moreover, the rheological properties of soybean oil, as well as partially and fully hydrogenated soybean oil, were determined (Ahmed et al., 2020).

Rheological properties and texture in bakery shortening and margarine directly affect the quality aspects, physical appearance, sensory evaluation, and texture of baked goods as finished products (Saghafi et al., 2019). A comparison of lipid shortening application as a function of molecular ensemble and shear showed that changes in melting and crystallization behavior of

shortening systems could be significantly affected by manipulating the amounts of triacylglycerols containing specific fatty acids (Humphrey and Narine, 2004).

Investigating the effect of the crystallization regime on the macroscopic rheological and sensory properties of shortening was the aim of this study. Through working on a fixed formulation, it was attempted to determine the extent of the influence of crystallization process parameters on the final shortening texture, as well as storage and elastic attributes. The effects of the cooling rate, agitation, and filling temperature on the functional properties of shortenings including adhesiveness, hardness, plasticity, and homogeneity as well as the storage modulus (G') and loss modulus (G") were assessed. Although there have been few studies in which the fat mixture composition with or without considering an isolated crystallization factor has been investigated, the main focus of the current work was the crystallization process parameters and their interactions, which have never been investigated in similar research.

2. Materials And Methods

A multipurpose bakery shortening was selected in order to investigate the effect of the cooling rate and mixing on shortening sensory, storage, and elastic moduli. The concerned shortening contained a chemically interesterified fat blend, which included 4.2% canola oil, 71.8% palm oil, and 24% fully hydrogenated sunflower oil. The final shortening formulation was as follows: 33.25% chemically interesterified fat blend, 11.25% fully hydrogenated sunflower oil, 3.75% canola oil, and 51.75% palm oil. Design-Expert (version 12) software was employed to determine the experiment crystallization factor runs and to fit the response models through response surface methodology. The design type and model were Box-Behnken and quadratic, respectively. Because of some technical limitations, 17 runs were agreed on accordingly, all of which were related to one block. The experimental design with coded values and actual percentages and ranges of levels for independent variables of the crystallization process are mentioned in Table 1. In order to stay within a reasonable number of test runs, three process parameters were selected as the main indicators of the crystallization circumstances. The concerned crystallization arrangement contained four cooling units and four kneading units as shown in Fig. 1. Samples of the studied shortening were prepared in a Gerstenberg and Agger crystallizer (1 + 1 + 1 + 1 Perfector 250/NH_3). The unit consists of a melting container, a chilling system (four separate chilling units), and a pin worker. Table 2 shows the parameters of the applied crystallization runs. The crystallization system fat inlet temperature was kept constant (65 ± 1°C). The sensory analysis of shortening samples was carried out by a panelist team consisting of 15 experts who had been trained before the test for the expected performance. In this regard, four descriptive attributes including texture adhesiveness, hardness, plasticity, and homogeneity were assessed accordingly. The sensory evaluation test and analysis were carried out a week after packaging during which shortening samples were kept at 16°C.

Table 1
Experimental ranges and levels of independent variables used in quadratic Box-Behnken response surface design

Factor	Symbol	Unit	Type	Range of Levels				Mean	Standard Deviation
				Low actual	Low coded	High actual	High coded		
Cooling Unit No. 3 Outlet Shortening Temperature	T_3	°C	Numeric	28	-1	31	+ 1	29.5	1.06
Kneading Unit 2 Intensity	RPM	Round per minute	Numeric	100	-1	280	+ 1	190	63.64
Filling Temperature	FT	°C	Numeric	30	-1	36	+ 1	33	2.12

Table 2
Crystallization treatments

Crystallization Treatments	Cooling Unit No. 3 Outlet Shortening Temperature °C	Kneading Unit 2 Intensity Round per minute	Filling Temperature °C
T1	29.5	280.0	30.0
T2	31.0	190.0	36.0
T3	31.0	280.0	33.0
T4	29.5	100.0	30.0
T5	28.0	280.0	33.0
T6	29.5	280.0	36.0
T7	28.0	190.0	36.0
T8	31.0	100.0	33.0
T9	31.0	190.0	30.0
T10	28.0	190.0	30.0
T11	28.0	100.0	33.0
T12	29.5	190.0	33.0
T13	29.5	100.0	36.0
T14	29.5	190.0	33.0
T15	29.5	190.0	33.0
T16	29.5	190.0	33.0
T17	29.5	190.0	33.0

In this descriptive study, data were obtained in the rheology lab of the National Nutrition and Food Technology Research Institute, Tehran, Iran. Rheological measurements were performed with a Physica MCR 301 rheometer (Anton-Paar, GmbH, Graz, Austria). Temperature control was carried out using a Peltier system equipped with a fluid circulator. The authors decided to perform rheological tests at 25°C which is common as the confectionary workshop temperature.

For all the samples, parallel plate (PP40/S-SN 16891; d = 2 mm) geometry was utilized. Data analysis was carried out using Rheoplus software (version 3.21) (Anton Paar, Graz, Austria). Strain sweep tests were performed (0.001-500%, 6.28 rad/s) to determine the limiting value of the linear viscoelastic range (LVE). To provide a direct view of whether the samples behaved as liquids or solids, loss tangent (ratio of loss modulus to elastic modulus) was calculated at the LVE region. The crossover point (G'=G") was also obtained. Frequency sweep tests were performed using a frequency ramp from 0.0628 to 126 rad/s. G' and G" in three angular frequencies of 0.0628, 3.31, and 126 (rad/s) were calculated as representatives of low, moderate, and high angular frequencies, respectively.

3. Results And Discussion

3.1. Sensory evaluation

According to Table 3, which reports the outcomes of four chosen qualitative attributes of the studied shortening samples, crystallization treatments number 3 and 7 possessed the most favorable overall functional sensory quality. Regarding the concerned shortening applications, the goal was to reach the highest possible plasticity and homogeneity while the adhesiveness needed to be minimum. The desired hardness for this shortening was recognized by expert assessors as favorable.

Table 3
Sensory evaluation outcomes at 16°C

Crystallization Run	Tempering Conditions	Adhesiveness	Hardness	Plasticity	Homogeneity	Overall Verdict
1	16°C	4 ± 1.2	3 ± 1.1	2 ± 1.1	2 ± 1.3	
2	More than One Week	4 ± 1.2	2 ± 1.3	3 ± 1.2	3 ± 1.1	
3		2 ± 1.1	3 ± 1.2	3 ± 1.1	3 ± 1.2	Superior Quality (+++)
4		3 ± 1.3	4 ± 1.1	2 ± 1.3	2 ± 1.2	
5		5 ± 1.1	2 ± 1.3	2 ± 1.3	4 ± 1.1	
6		1 ± 1.3	4 ± 1.2	3 ± 1.3	3 ± 1.3	
7		4 ± 1.1	4 ± 1.2	3 ± 1.1	3 ± 1.3	Overall Acceptable (++)
8		3 ± 1.2	4 ± 1.3	2 ± 1.1	3 ± 1.3	
9		2 ± 1.3	4 ± 1.1	4 ± 1.3	2 ± 1.2	
10		2 ± 1.2	4 ± 1.3	3 ± 1.1	2 ± 1.1	Overall Acceptable (++)
11		3 ± 1.1	4 ± 1.2	2 ± 1.2	5 ± 1.3	Overall Acceptable (++)
12		4 ± 1.2	4 ± 1.1	2 ± 1.2	3 ± 1.3	
13		2 ± 1.3	4 ± 1.2	2 ± 1.3	5 ± 1.1	
14		4 ± 1.3	4 ± 1.2	2 ± 1.1	3 ± 1.3	
15		4 ± 1.2	4 ± 1.1	2 ± 1.2	3 ± 1.3	
16		4 ± 1.1	4 ± 1.2	2 ± 1.1	3 ± 1.3	
17		4 ± 1.3	4 ± 1.1	2 ± 1.2	3 ± 1.3	

Note: Mean Values ± SD (n = 3).

3.2. Rheological characterization

Figure 2 depicts the strain sweep rheograms related to the crystallization treatments. For the G’ of 17 crystallization treatments, it was possible to discriminate two different regions, namely, a small linear viscoelastic region, in which G’ was nearly constant and a bigger nonlinear region, in which G’ started to diminish with increasing strain. The LVE region was determined in order to help distinguish between the strong and weak structures of the samples. As can be seen in Table 4, the LVE region was greater in sample 4. For most solid foods, LVE is between 0.1% and 2%; however, in this study, we chose the strain of 0.05% in the LVE region. In the case of G”, the behavior of samples in the strain sweep test was identical to the one mentioned for G’. In all the samples, both moduli finally tended to crossover; therefore, all 17 crystallization treatments showed flow points. As shown at lower strains, G’ values were sensibly greater than G” values. While with increasing strain percentages, G” values were ultimately greater than G’ values. Due to the fact that in all the cases, before the flow point, G’ was higher than G” it can be concluded that all the samples in the linear viscoelastic region showed a solid-like behavior. However, at higher strains, G” was higher and the samples exhibited a more liquid-like behavior. The strain sweep parameters of 17 cases are listed in Table 4. G_f is the amount of the stress at the crossover point and indicates that exerting further stress resulted in the structure breakdown and thus the flow of the matter (Naeli et al., 2022). After this point, G" is more than G' (tan (δ) > 1), which suggests a structure rupture and the start of the flow behavior. The highest amount of G_f was observed in sample 9. $Tan(\delta)_{LVE}$ is the G' to G" ratio in the LVE region, and this parameter can be an indicator of the physical properties of the manufactured samples. According to the reported data in Table 4, samples 1 and 2 had the lowest amount of $Tan(\delta)_{LVE}$.

Table 4
Strain sweep parameters of 17 crystallization treatments at 25°C. Further rheological experiments were performed at the mentioned temperature, limiting value of linear viscoelastic range γ_l (%), damping factor for the end of LVE region (tan δ_{Lve}), and crossover point G_f (pa) (G'=G")

Crystallization Treatments	γ_l (%)	Tan δ_{Lve}	G_f (Pa)
T1	0.0513	0.1060	400.00
T2	0.0596	0.0703	1240.00
T3	0.0650	0.0833	2165.30
T4	0.2950	0.1932	1171.10
T5	0.0701	0.1920	741.28
T6	0.1060	0.1290	24714.00
T7	0.0932	0.1260	2459.70
T8	0.0799	0.1490	1740.40
T9	0.0972	0.1340	4398.90
T10	0.0595	0.1290	2760.20
T11	0.0619	0.1040	3578.70
T12	0.0598	0.0953	1965.70
T13	0.0605	0.1080	13051.00
T14	0.0701	0.192	741.28
T15	0.0701	0.192	741.28
T16	0.0701	0.192	741.28
T17	0.0701	0.192	741.28

Strain sweep curves for rheology parameters, such as G', G", and the loss tangent of an all-purpose shortening crystallized with and without high-intensity ultrasound were studied in a similar investigation, which showed similar G' and G" profiles after 60 min of crystallization and during storage at 25°C (Lee, Marsh, and Martini, 2020). A comparable work reported that during crystallization, the rheology of the fats changed from a weak viscoelastic solid system to a weak viscoelastic liquid. In this examination, it appeared that, initially, the rheology was dominated by the few large crystals present, but after longer stirring, weak viscoelastic liquid behavior, which is characteristic of liquid slip planes between solid crystals, dominated the behavior (Bell et al., 2007). Additionally, storage and loss moduli changes of binary combinations of canola oil and palm stearin were assessed in a study intended for zero-trans cake shortening formulation and characterization. The rheological results of this work showed patterns compatible with the current study (Saghafi et al., 2018).

Considering the strain sweep, frequency sweep tests were performed, and the mechanical spectra of the cases are depicted in Fig. 3. Table 5 presents the viscous and elastic moduli of 17 samples in three angular frequencies of 0.0628, 3.31, and 126 rad/s. The results of the frequency sweep test revealed that G' modulus was greater than G" modulus in all frequency ranges and no crossover was observed. It is known that in gel systems, G' is greater than G" in the applied frequency range. According to the frequency sweep data, a solid-like behavior was observed in all frequency ranges. This behavior represents a strong network as a result of forming the corresponding network structure.

Table 5
Frequency sweep parameters of 17 crystallization treatments, G’ (Pa), and G” (Pa) of each run in frequency sweep test was calculated in three angular frequencies, namely, high ω = 126 (rad/s), medium ω = 3.31) rad/s) and low = 0.628 (rad/s) angular frequencies

Crystallization Treatments	Storage Modulus, G' (Pa)/100000			Loss Modulus, G" (Pa)/100000			Tan δ		
	ω= (0.0628)	ω= (3.31)	ω= (126)	ω= (0.0628)	ω= (3.31)	ω= (126)	ω= (0.0628)	ω= (3.31)	ω= (126)
T1	0.507	0.947	1.21	0.359	0.24	0.265	0.7	0.3	0.2
T2	8.64	9.56	11.1	2.1	1.44	1.22	0.2	0.2	0.1
T3	9.48	10.1	11.6	1.85	1.4	1.17	0.2	0.1	0.1
T4	9.77	10.6	12.1	1.97	1.4	1.22	0.2	0.1	0.1
T5	1.89	2.24	2.69	0.644	0.465	0.484	0.3	0.2	0.2
T6	8.85	10.2	11.8	2.09	1.36	1.24	0.2	0.1	0.1
T7	11.4	12.4	14.3	2.68	1.89	1.52	0.2	0.2	0.1
T8	5.95	7.0	8.25	1.63	1.21	1.05	0.3	0.2	0.1
T9	7.0	8.27	9.59	1.95	1.1+	1.01	0.3	0.1	0.1
T10	5.24	5.92	6.91	1.3	1.02	0.911	0.2	0.2	0.1
T11	10.9	12.5	14.4	2.86	1.78	1.45	0.3	0.1	0.1
T12	11.4	12.1	13.9	2.46	1.77	1.36	0.2	0.1	0.1
T13	8.26	9.8	11.5	2.18	1.37	1.25	0.3	0.1	0.1
T14	11.4	12.1	13.9	2.46	1.77	1.36	0.2	0.1	0.1
T15	11.4	12.1	13.9	2.46	1.77	1.36	0.2	0.1	0.1
T16	11.4	12.1	13.9	2.46	1.77	1.36	0.2	0.1	0.1
T17	11.4	12.1	13.9	2.46	1.77	1.36	0.2	0.1	0.1

3.3. Fitting for the best model

Statistical analysis parameters of the Fisher test value (F-value), the p-value of model, coefficient of determination (R^2), the adjusted coefficients of determination (R^2-adj), predicted R^2, the p-value of lack of fit (LOF), adequate precision, and percentage of the coefficient of variation (CV%) obtained from the analysis of variance (ANOVA) were used for evaluating the goodness of fit in models. Fitted quadratic equations were applied for achieving the optimized formulation. Statistical significance of the model parameters was set at 5% (p-value = 0.05). Tables 4 and 5 report the corresponding 17-run obtained responses. All of the responses were fitted to the quadratic model. According to Table 6, the p-value for the model indicates that the models are significant at less than a 0.05 level.

Table 6
Parameter estimates and analysis of variance for responses model*

Response	Model		Fit Statistics								
	F-value	p-value	Sum of Squares	Mean Square	df	R^2	Adjusted R^2	Standard Deviation	Mean	Adequate precision	CV %
G' (0.0628 rad/s)	152.09	< 0.0001	5401.87	600.21	9	0.9949	0.9884	1.99	22.88	33.9401	8.68
G' (3.31 rad/s)	34.92	< 0.0001	278.97	31.00	9	0.9782	0.9502	0.9421	7.09	15.4673	13.28
G' (126 rad/s)	31.44	< 0.0001	362.43	40.27	9	0.9759	0.9448	1.13	8.24	14.7008	13.73
G" (0.0628 rad/s)	23.88	0.0002	10.48	1.16	9	0.9685	0.9279	0.2209	1.57	13.3543	14.09
G"(3.31 rad/s)	29.23	< 0.0001	4.62	0.5133	9	0.9741	0.9408	0.1325	1.08	15.6810	12.27
G" (126 rad/s)	16.57	0.0006	2.56	0.2846	9	0.9552	0.8975	0.1311	0.9462	11.3342	13.85

*P < 0.05 is significant.

3.4. Storage and loss moduli

The equations of predicted models are presented in Table 7. The concerned regression equations predict the value of each response variable when the independent factors are varied; a positive sign in front of the terms suggests a synergistic effect, whereas a negative sign indicates an antagonistic effect.

Table 7
Final equation of responses

Response	Equations (X_1: T3, X_2: RPM, X_3: FT)
G' (0.0628 rad/s)/100000	$+ 5886.56945-151.23892X_1-0.848513X_2-209.69818X_3 + 0.10492X_1X_2 + 0.100633X_1X_3 - 0.000013X_2X_3 + 2.3769X_1^2 + 0.001149X_2^2 + 3.11504X_3^3$
G' (3.31 rad/s)/100000	$+ 1394.30199-38.21195X_1-0.003948X_2-48.95159X_3- 0.003469X_1X_2 + 0.028333X_1X_3 - 0.000741X_2X_3$ $0.624278X_1^2 + 0.00029X_2^2 + 0.729208X_3^3$
G' (126 rad/s)/100000	$+ 1589.50194-43.29593X_1 + 0.002218X_2-56.09968X_3 - 0.004352X_1X_2 + 0.038333X_1X_3 - 0.000741X_2X_3 + 0.705556X_1^2 + 0.000335X_2^2 + 0.832778X_3^3$
G" (0.0628 rad/s)/100000	$+ 269.99817-6.403457X_1 + 0.024624X_2-10.57241X_3 - 0.001335X_1X_2 + 0.031111X_1X_3 - 0.000287X_2X_3 + 0.092944X_1^2 + 0.000053X_2^2 + 0.146875X_3^3$
G"(3.31 rad/s)/100000	$+ 188.44778-5.62574X_1 + 0.015144X_2-6.27875X_3 - 0.001093X_1X_2 + 0.011667X_1X_3 + 2.56834\ E\ (-18)X_2X_3 + 0.0900X_1^2 + 0.000037X_2^2 + 0.089444X_3^3$
G" (126 rad/s)/100000	$+ 133.80472-3.79015X_1 + 0.018788X_2-4.67701X_3 - 0.000974X_1X_2 + 0.005000X_1X_3 - 0.000074X_2X_3 + 0.062778X_1^2 + 0.000028X_2^2 + 0.068583X_3^3$

Figure 4 demonstrates storage and loss moduli models in high angular frequency (ω = 126 rad/s) when the filling temperature is 33°C. Figure 5 indicates storage and loss moduli (at the angular velocity of 126 rad/s) when the concerned crystallization

parameters deviate from a reference point where all three crystallization factors are at their mean values (i.e., T_3 = 29.5°C, RPM = 190, and FT = 33°C).

3.5. Optimized crystallization treatment

According to Table 3, the shortening sample with the most favorable sensory properties was related to crystallization treatment number 3 (i.e., T_3 = 31°C, RPM = 280, and FT = 33°C). At the mentioned related parameters, all the modeled storage and loss moduli (i.e., G' and G" at 0.0628, 3.31, and 126 rad/s) were in the minimum values range. As an example, Fig. 6 demonstrates the storage and loss moduli in the lower range of angular velocity (i.e., G' and G" at 0.0628 rad/s).

As another illustrative example, Fig. 7 shows the storage and loss moduli changes at the middle angular velocity (i.e., 3.31 rad/s) when RPM is 280. In a similar fashion, the crystallization process conditions related to the most desirable functional properties correspond to the minimum storage and loss moduli values.

One of the current study's main objectives was to achieve a comprehensive model for consequent optimization activities regarding the determination of the proper crystallization parameters for different shortening functional requirements. As discussed earlier, the most favorable functional properties of the concerned shortening correspond to minimum storage and loss moduli values. The chosen optimization criteria and the achieved solutions are summarized in Table 8.

Table 8 Optimization criteria and solution

Optimization Criteria				**Solution (Desirability=0.94)**			
Response	**Goal**	**Lower Limit**	**Upper Limit**	**Factor**		**Response value**	
G' (0.0628 rad/s)/100000	minimize	0.507	11.4			G' (0.0628 rad/s)/100000	0.845
G' (3.31 rad/s)/100000	minimize	0.947	12.5			G' (3.31 rad/s)/100000	1.383
G' (126 rad/s)/100000	minimize	1.21	14.4			G' (126 rad/s)/100000	1.749
G" (0.0628 rad/s)/100000	minimize	0.359	2.86	T3	30.4	G" (0.0628 rad/s)/100000	0.512
G" (3.31 rad/s)/100000	minimize	0.24	1.89	RPM	228	G"(3.31 rad/s)/100000	0.349
G" (126 rad/s)/100000	minimize	0.265	1.52	FT	33.1	G" (126 rad/s)/100000	0.406

Hence, these responses are considered in the range of the studied levels. Derringer's desirability function also calculated the optimum conditions:

$$D = \sqrt[m]{d_1 d_2 \ldots d_m}$$

Equation 1. Derringer's desirability function

where m is the number of responses studied in the optimization process, and d is the individual desirability function of each response. Derringer's desirability function (D) can take values from 0 to 1. A value greater than 0.7 indicates that the combination of the different criteria is matched in a global optimum (Bezerra et al., 2008; Ramsay et al., 2014).

To validate the optimization results, three replicates of the experiments for each response were performed under optimal conditions. When optimum circumstances were applied, the comparison of the experimental results with the predicted ones was carried out using paired t-test (Table 9). As indicated, insignificant differences between the experimental and predicted results imply the validity of the optimal outcomes.

Table 9
Results of validity evaluation of optimal parameters

Response	Predicted value	Experimental value	p-value (paired-t test)
G' (0.0628 rad/s)/100000	0.845 ± 1.162	0.923 ± 0.765	0.62
G' (3.31 rad/s)/100000	1.382 ± 1.104	1.397 ± 0.665	0.96
G' (126 rad/s)/100000	1.748 ± 1.330	2.135 ± 0.804	0.25
G" (0.0628 rad/s)/100000	0.512 ± 0.309	0.779 ± 0.435	0.62
G"(3.31 rad/s)/100000	0.349 ± 0.191	0.334 ± 0.245	0.84
G" (126 rad/s)/100000	0.405 ± 0.179	0.335 ± 0.245	0.42

4. Conclusion

There is growing interest regarding the relationship between crystallization parameters, and rheological and functional properties of different bakery and confectionary shortenings. There are several studies available in which rheological, functional, and sensory attributes of some fat and oil blends (including margarine and shortening product applications) have been reported. Rarely in these works, the effects of crystallization process parameters have been the main focus of the investigation. On the other hand, the current study's principal emphasis was to determine the impacts of crystallization arrangement and parameters on the resultant shortening. Here, it was shown that the storage and loss moduli of a fat mixture were altered considerably when the selected crystallization process parameters were manipulated. The storage and loss moduli values demonstrated similar patterns when crystallization parameters were altered. By applying the desired criteria, the optimum values of the third cooling stage outlet temperature, kneading intensity, and filling temperature were 30.4°C, 228, and 33.1°C, respectively. The following validity evaluation confirmed the emerged optimized factors which underlines the vital role of similar approaches for understanding, modeling, and predicting different shortening rheological behaviors.

Declarations

Acknowledgment

The authors gratefully acknowledge the supports of Margarine Manufacturing Company.

Author information

Affiliations

1. Ph.D. Student, Department of Food Science and Technology, Tabriz Branch, Islamic Azad University, Tabriz, Iran
2. Associate Professor, Department of Food Science and Technology, Tabriz Branch, Islamic Azad University, Tabriz, Iran
3. Corresponding author: Assistant Professor, Department of Food and Nutrition Policy and Planning Research. National Nutrition and Food Technology Research Institute. Faculty of Nutrition and Food Science. Shahid Beheshti University of Medical Sciences and Health Services, Email: zargaran@sbmu.ac.ir
4. Professor, Proteomics Research Center and Department of Biostatistics, Faculty of Allied Medical Sciences, Shahid Beheshti University of Medical Sciences, Tehran, Iran

Mahnaz Ameli[1], Leila Roufegarinejad [2], Azizollaah Zargaraan[3 *], Farid Zayeri[4]

Contributions

MA designed and performed all of the experiments. She also wrote the draft of the manuscript. LR designed the research and analyzed the results of the experiments. AZ designed the rheological tests and analyzed the results. FZ performed all of the

modeling procedures and their analyzes.

Corresponding author

Correspondence to Azizollaah Zargaraan (aziz.zargaran@gmail.com)

Conflict of interest

The authors declare that they have no known competing financial interests or personal relationships that could have appeared to influence the work reported in this paper.

Funding:

This research received no specific grant from any funding agency in the public, commercial, or not-for-profit sectors.

References

1. Ahmadi, L., and A. G. Marangoni. 2009. “Functionality and Physical Properties of Interesterified High Oleic Shortening Structured with Stearic Acid.” *Food Chemistry* 117(4):668–73.
2. Ahmed, Ibtesam I., Manal A. Sorour, Mohamed S. Abbas, and Amira Sh Soliman. 2020. “Physiochemical Properties of a Model Shortening with Trans-Free and Low-Saturated Fatty Acid.” *Journal of Advanced Pharmacy Education \& Research| Jul-Sep* 10(3):35.
3. Alexandersen, Klaus A., Saeed M. Ghazani, and Alejandro G. Marangoni. 2020. “Margarine Processing Plants and Equipment.” *Bailey’s Industrial Oil and Fat Products* 1–64.
4. Bell, A., M. H. Gordon, W. Jirasubkunakorn, and K. W. Smith. 2007. “Effects of Composition on Fat Rheology and Crystallisation.” *Food Chemistry* 101(2):799–805.
5. Bezerra, Marcos Almeida, Ricardo Erthal Santelli, Eliane Padua Oliveira, Leonardo Silveira Villar, and Luciane Amélia Escaleira. 2008. “Response Surface Methodology (RSM) as a Tool for Optimization in Analytical Chemistry.” *Talanta* 76(5):965–77.
6. Erickson, David R. 1990. *Edible Fats and Oils Processing: Basic Principles and Modern Practices: World Conference Proceedings*. The American Oil Chemists Society.
7. Haighton, A. J. 1969. “Margarine Oil Formulation and Control.” *Journal of the American Oil Chemists Society* 46(10):570.
8. Hakimzadeh, Vahid, Raheleh Mahjoob, Ataye Salehi, and Jamshid Farmani. 2020. “Production and Evaluation of Physicochemical and Rheological Properties of Sorbitan Mono-Stearate and Sorbitan Tri-Stearate Based Oleogels as Low SFA Shortening.” 1–12.
9. Humphrey, K. L., P. H. L. Moquin, and S. S. Narine. 2003. “Phase Behavior of a Binary Lipid Shortening System: From Molecules to Rheology.” *JAOCS, Journal of the American Oil Chemists’ Society* 80(12):1175–82.
10. Humphrey, K. L., and S. S. Narine. 2004. “A Comparison of Lipid Shortening Functionality as a Function of Molecular Ensemble and Shear: Crystallization and Melting.” *Food Research International* 37(1):11–27.
11. Lee, Juhee, Melissa Marsh, and Silvana Martini. 2020. “Effect of Storage Time on Physical Properties of Sonocrystallized All-Purpose Shortening.” *Journal of Food Science* 85(10):3391–99.
12. Litwinenko, J. W., A. M. Rojas, L. N. Gerschenson, and A. G. Marangoni. 2002. “Relationship Between Crystallization Behavior, Microstructure, and Mechanical Properties in a Palm Oil-Based Shortening.” *JAOCS, Journal of the American Oil Chemists’ Society* 79:647–54.
13. Masuchi, Monise Helen, Kelly Moreira Gandra, André Luis Marangoni, Cristiane De Sá Perenha, Ming Chih Chiu, Renato Grimaldi, and Lireny Aparecida Guaraldo Gonçalves. 2014. “Fats from Chemically Interesterified High-Oleic Sunflower Oil and Fully Hydrogenated Palm Oil.” *JAOCS, Journal of the American Oil Chemists’ Society* 91(5):859–66.
14. Moriya, Yuzuki, Yoshimune Hasome, and Kiyoshi Kawai. 2020. “Effect of Solid Fat Content on the Viscoelasticity of Margarine and Impact on the Rheological Properties of Cookie Dough and Fracture Property of Cookie at Various

Temperature and Water Activity Conditions." *Journal of Food Measurement and Characterization* 14(6):2939–46.

15. Naeli, Mohammad Hossein, Jafar M. Milani, Jamshid Farmani, and Azizollaah Zargaraan. 2022. "Developing and Optimizing Low-Saturated Oleogel Shortening Based on Ethyl Cellulose and Hydroxypropyl Methyl Cellulose Biopolymers." *Food Chemistry* 369:130963.
16. Nguyen, Viet, Tom Rimaux, Vinh Truong, Koen Dewettinck, and Filip Van Bockstaele. 2021. "The Effect of Cooling on Crystallization and Physico-Chemical Properties of Puff Pastry Shortening Made of Palm Oil and Anhydrous Milk Fat Blends." *Journal of Food Engineering* 291(May 2020):110245.
17. Ramsay, Aina, Ophélie Fliniaux, Jingjing Fang, Roland Molinie, Albrecht Roscher, Eric Grand, Xavier Guillot, José Kovensky, Marc André Fliniaux, Bernd Schneider, and François Mesnard. 2014. "Development of an NMR Metabolomics-Based Tool for Selection of Flaxseed Varieties." *Metabolomics* 10(6):1258–67.
18. Saghafı, Zahra, Mohammad Hossein Naeli, Mahnaz Tabibiazar, and Azizollaah Zargaraan. 2018. "Zero-Trans Cake Shortening: Formulation and Characterization of Physicochemical, Rheological, and Textural Properties." *JAOCS, Journal of the American Oil Chemists' Society* 95(2):171–83.
19. Saghafı, Zahra, Mohammad Hossein Naeli, Mahnaz Tabibiazar, and Azizollaah Zargaraan. 2019. "Modeling the Rheological Behavior of Chemically Interesterified Blends of Palm Stearin/Canola Oil as a Function of Physicochemical Properties." *JAOCS, Journal of the American Oil Chemists' Society* 96(11):1219–34.

Figures

Figure 1

Crystallization process cooling and kneading units arrangement

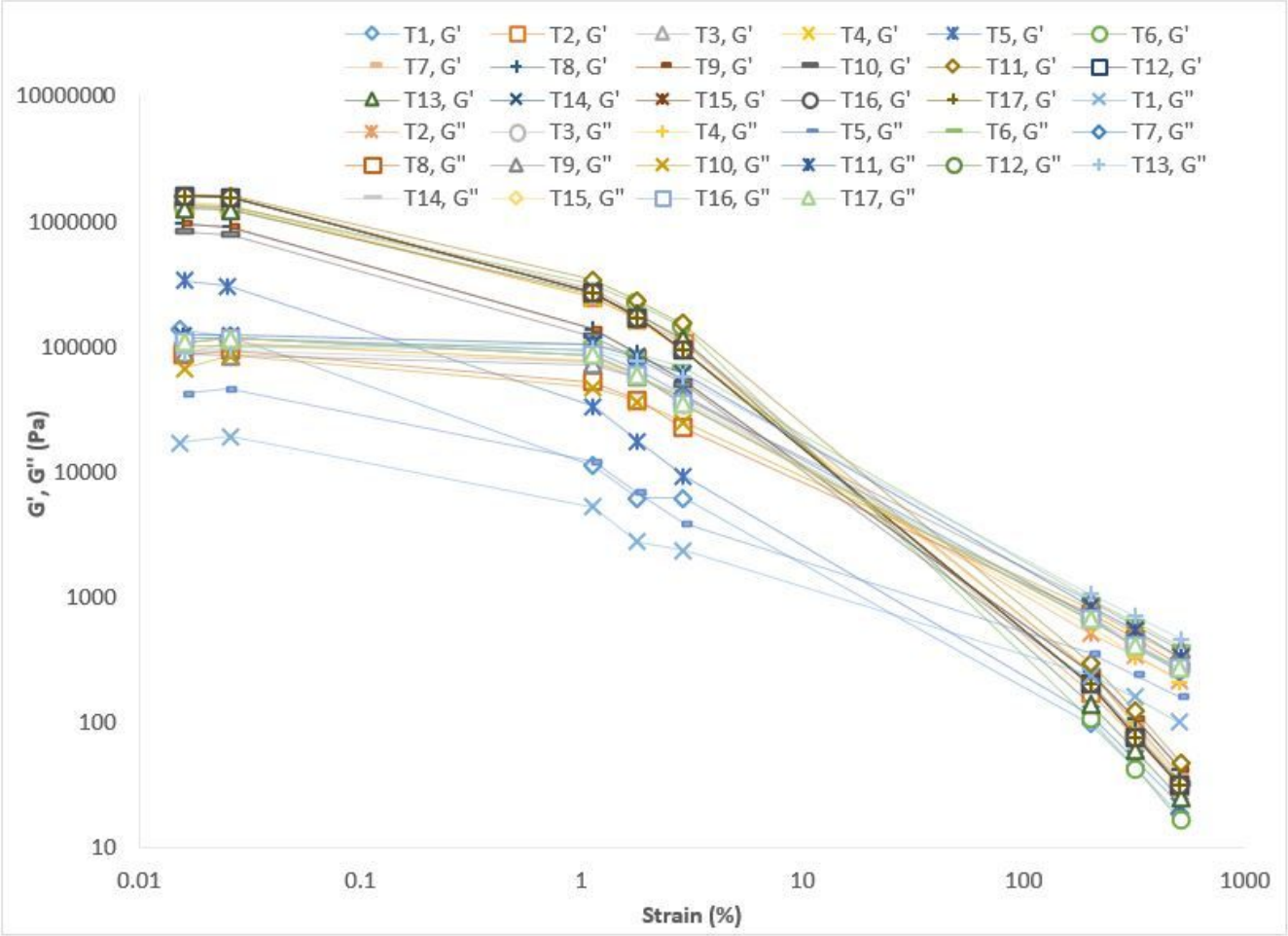

Figure 2

Strain sweep of the 17 crystallization treatments

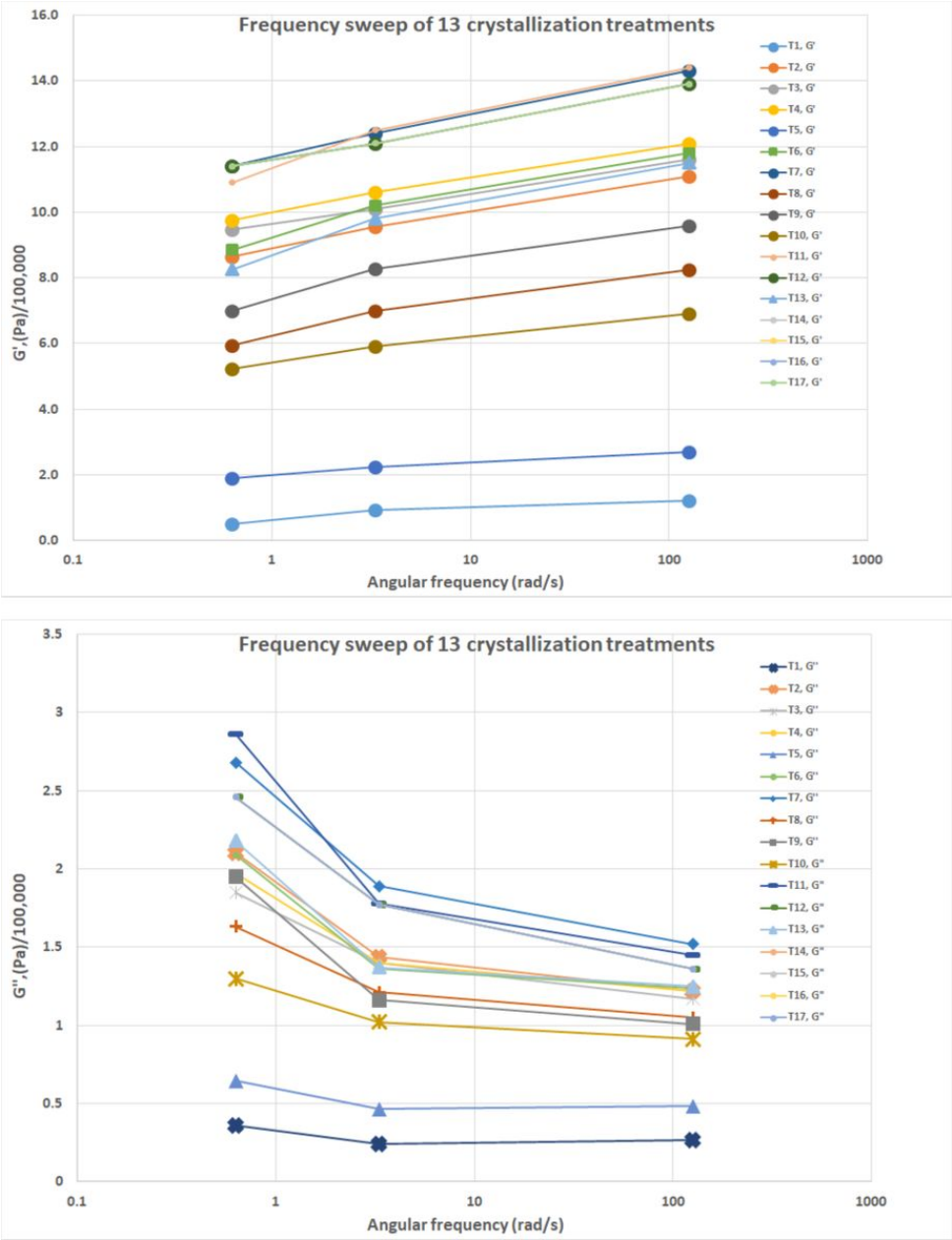

Figure 3

Frequency dependency of G’ (a) and G” (b) of the 17 crystallization treatments

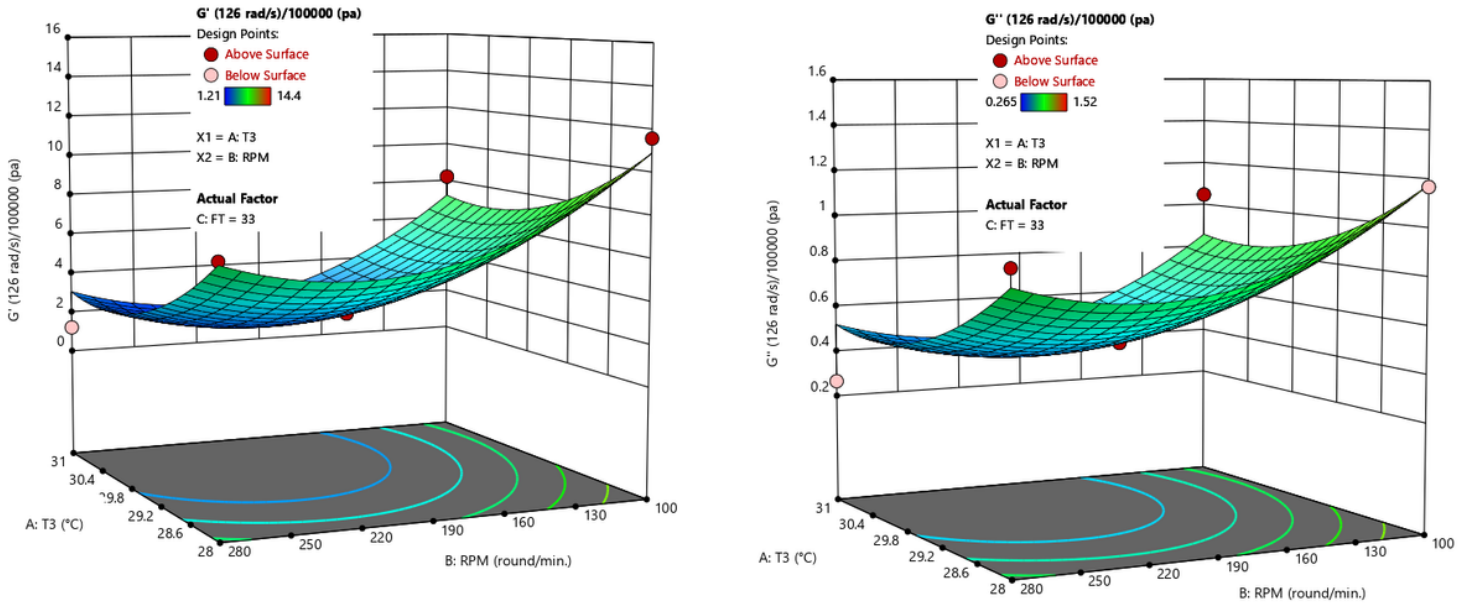

Figure 4

G’ and G” (126 rad/s) when filling temperature is 33°C

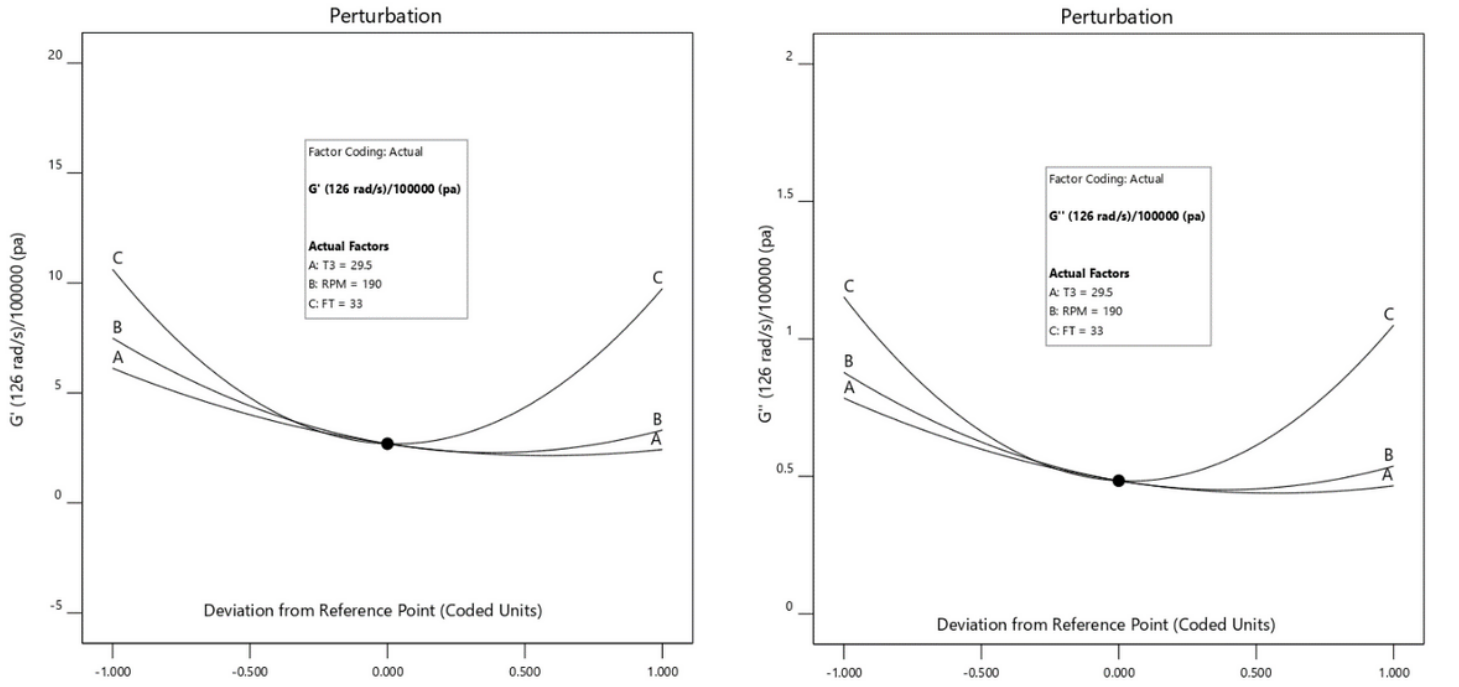

Figure 5

Perturbation diagram of G’ and G” (126 rad/s) when filling temperature is 33°C

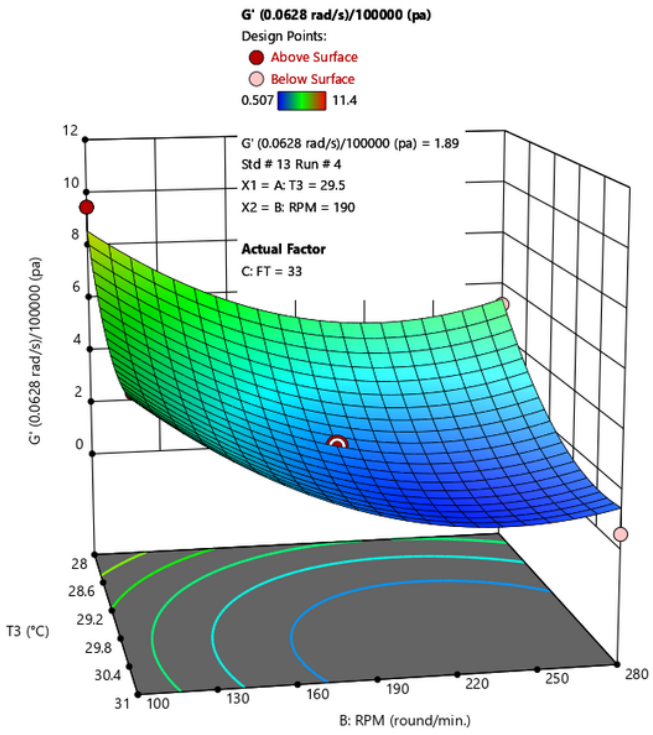

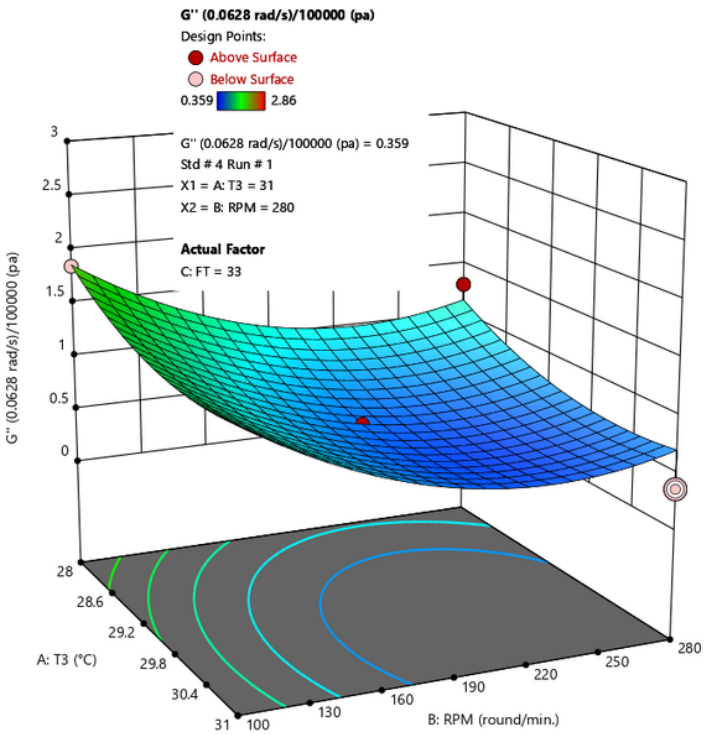

Figure 6

G’ and G” (0.0628 rad/s) when filling temperature is 33°C

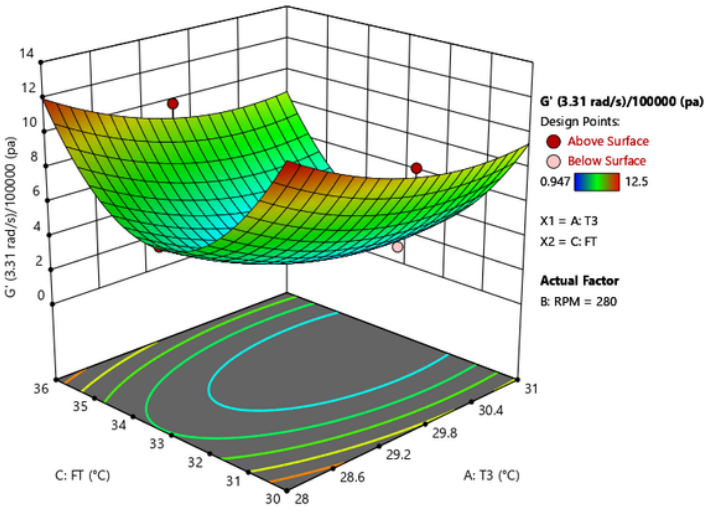

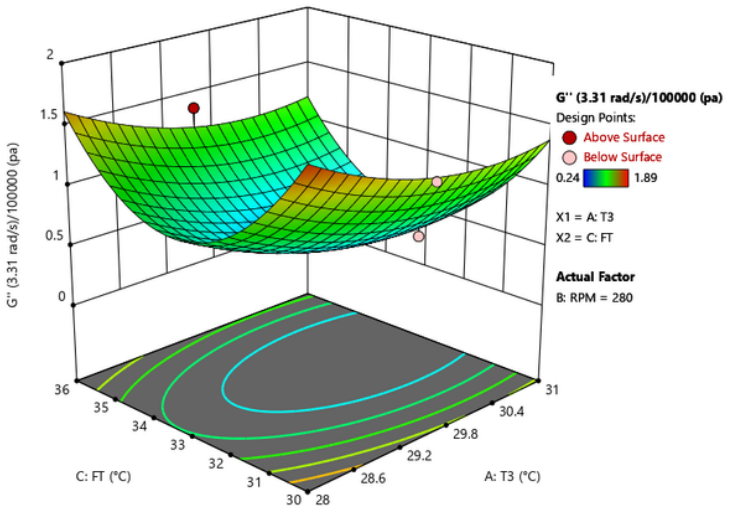

Figure 7

G’ and G” (3.31 rad/s) when RPM is 280